

Rare Leptonic B and $b \rightarrow s\ell^+\ell^-$ Decays at B-factories

Jack L. Ritchie (from the BABAR Collaboration)
University of Texas at Austin, Austin, Texas, USA

We review recent results from the BABAR and Belle experiments on rare electroweak B -meson decays, with emphasis on those occurring through flavor changing neutral current interactions of the type $b \rightarrow s\ell\bar{\ell}$. The recent results include measurements of the isospin asymmetry and lepton forward-backward asymmetry in $B \rightarrow K^*\ell^+\ell^-$ decays from BABAR, a search for $B \rightarrow \pi\ell^+\ell^-$ from Belle, and searches for $B \rightarrow K^{(*)}\nu\bar{\nu}$ from BABAR. We also briefly review the status of $B^0 \rightarrow \ell^+\ell^-$ and $B^+ \rightarrow \ell^+\nu$ searches.

I. INTRODUCTION

The study of flavor-changing neutral current (FCNC) decays has been a fruitful avenue of research throughout the history of particle physics. Today rare B -meson decays based on the process $b \rightarrow s\ell^+\ell^-$ (where $\ell = e$ or μ) provide one of the most promising probes for new physics. Both B -factory experiments, BABAR and Belle, have observed decays of this type and reported measurements which probe their underlying structure.

The decays proceed through loop diagrams such as those shown in Figure 1. The theoretical treatment

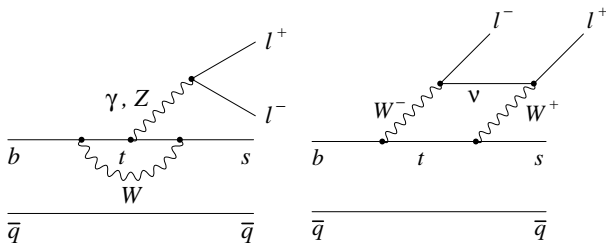


FIG. 1: The electroweak penguin (left) and W -box (right) diagrams responsible for $B \rightarrow K^{(*)}\ell^+\ell^-$ decays.

of $b \rightarrow s\ell^+\ell^-$ transitions in the Standard Model (SM) invokes an effective field theory in which the Hamiltonian is a sum of terms, where each term consists of CKM factors and a Wilson coefficient multiplying an operator that is formed from the light quark and lepton fields. The Wilson coefficients, obtained by integrating out the heavy particles, characterize the short-distance physics in these decays. New physics (e.g., SUSY) would modify the Wilson coefficients by providing new particles inside the loops and may modify the Hamiltonian by adding scalar or pseudoscalar terms. To account for QCD effects that mix the operators, so-called effective Wilson coefficients are defined, which are functions of a renormalization scale μ (typically taken to be 4.6 GeV in the \overline{MS} scheme) and the squared dilepton mass $q^2 = m_{\ell\bar{\ell}}^2$. Measurements of $b \rightarrow s\ell^+\ell^-$ decays mainly probe the effective Wilson coefficients \tilde{C}_7 , \tilde{C}_9 , and \tilde{C}_{10} . Fully inclusive measurements are not possible, and the background environment is very difficult for analyses that com-

bine multiple exclusive modes, so it is conventional to focus on the exclusive modes $B \rightarrow K\ell^+\ell^-$ and $B \rightarrow K^*\ell^+\ell^-$ (denoted together as $B \rightarrow K^{(*)}\ell^+\ell^-$). Form factor uncertainties complicate the interpretation of exclusive measurements, but a number of measurable asymmetries, defined below, are relatively insensitive to these uncertainties. An up-to-date summary of the theoretical status, along with extensive references, can be found in Ref.[1].

The related decays $B \rightarrow K^{(*)}\nu\bar{\nu}$ are also of considerable interest, but experimentally present almost insurmountable problems owing to the missing neutrinos. Nonetheless, the B -factory experiments have conducted searches, and BABAR has a recent update.

The decays $B \rightarrow \pi\ell^+\ell^-$ and $B^0 \rightarrow \ell^+\ell^-$ proceed through essentially the same diagrams, where the s quark is replaced by a d quark, leading to CKM suppression by a factor $|V_{td}/V_{ts}|^2 \simeq 0.04$; in addition, the two-body decays are helicity suppressed. Consequently, these decays have quite small SM branching fractions and have thus far not been observed. Belle has recently reported a new limit on $B \rightarrow \pi\ell^+\ell^-$.

The decays $B^+ \rightarrow \ell^+\nu$ proceed through simple W -exchange and are sensitive to the product $f_B|V_{ub}|$. Combined with a measurement of $|V_{ub}|$ from another source, measurement of any of these branching fractions would provide a good measurement of the B -meson decay constant f_B . For the $\ell = \mu$ and e cases, the branching fractions are quite small due to helicity suppression, although the $B^+ \rightarrow \mu^+\nu$ decay appears to be only just beyond the reach of the current B -factory experiments. The status of $B^+ \rightarrow \tau^+\nu$ is presented in another contribution to this conference [2].

Below, the status of these rare FCNC B decays is described, with emphasis on recent results from Belle and BABAR.

II. $B \rightarrow K^{(*)}\ell^+\ell^-$ MEASUREMENTS

These decays experience interference from the processes $B \rightarrow K^{(*)}J/\psi \rightarrow K^{(*)}\ell^+\ell^-$ and $B \rightarrow K^{(*)}\psi(2S) \rightarrow K^{(*)}\ell^+\ell^-$. Consequently, it is necessary to remove events with lepton-pair mass close to the J/ψ or $\psi(2S)$ peaks. On the positive side, these

processes provide large and well-understood control samples which can be used to study efficiencies and to study the characteristics of signal-like events (e.g., to determine PDFs for fits).

The main backgrounds to these decays arise from B and D semileptonic decays. The two leptons can come from the semileptonic decay of both the B and \bar{B} in an event, or from the semileptonic decays of a B and also its daughter D . These backgrounds are suppressed by combining event shape information, vertex information, and missing energy information into multivariate analysis techniques (such as neural nets). Another important background, $B \rightarrow D\pi$ (followed by $D \rightarrow K^{(*)}\pi$) wherein pions are misidentified as muons, can be explicitly vetoed by rejecting events in which one of the muons, when assigned the pion mass, reconstructs in combination with a kaon to the D mass. Signal can then be separated from the residual background using maximum likelihood fits, typically utilizing the differing shapes of signal and background distributions in the quantities $\Delta E = E_B^* - E_{\text{beam}}^*$ and $m_{ES}[\text{BABAR}] = m_{bc}[\text{Belle}] = \sqrt{E_{\text{beam}}^{*2} - p_B^{*2}}$, where E_B^* and p_B^* are the CM energy and momentum of the reconstructed B .

$BABAR$ has recently reported a series of measurements based on 349 fb^{-1} of data (384 million $B\bar{B}$ pairs). These results are described below and are compared to Belle results where possible.

The $BABAR$ analysis of $B \rightarrow K^{(*)}\ell^+\ell^-$ reconstructs 10 submodes, reflecting five possible $K^{(*)}$ final states (K^\pm , K_S^0 , $K^\pm\pi^\mp$, $K^\pm\pi^0$, and $K_S^0\pi^\pm$), each paired with e^+e^- or $\mu^+\mu^-$. Electrons (muons) are required to have $p > 0.3(0.7) \text{ GeV}/c$. Photons consistent with bremsstrahlung are combined with the associated electron. Two q^2 -bins are defined: a low- q^2 bin $0.1 < q^2 < 7.02 \text{ GeV}^2$ and a high- q^2 bin $q^2 > 10.24 \text{ GeV}^2$ but excluding $12.96 < q^2 < 14.06$ for the $\psi(2S)$. More q^2 bins are desirable, but are not possible with the current event sample. The so-called pole region ($q^2 < 0.1 \text{ GeV}^2$) is excluded due to the $1/q^2$ term in $B \rightarrow K^*\gamma$.

A. Branching Fractions

The values of the recent $BABAR$ branching fraction measurements, which combine both q^2 bins and lepton-pair cases, and includes correction for the excluded J/ψ and $\psi(2S)$ regions, are:

$$\mathcal{B}(B \rightarrow K\ell^+\ell^-) = (3.9 \pm 0.07 \pm 0.2) \times 10^{-7},$$

$$\mathcal{B}(B \rightarrow K^*\ell^+\ell^-) = (11.1_{-1.8}^{+1.9} \pm 0.7) \times 10^{-7}.$$

Figure 2 shows these results, along with prior measurements from other experiments and two theoretical results based on the SM. The experimental results are consistent with the SM predictions.

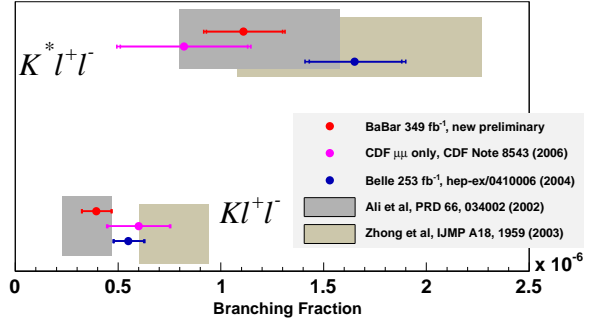


FIG. 2: Summary of branching fraction results from different experiments for $B \rightarrow K^{(*)}\ell^+\ell^-$.

B. Decay Asymmetries

By reconstructing 10 separate submodes for $B \rightarrow K^{(*)}\ell^+\ell^-$, it becomes possible to construct a variety of decay asymmetries which test different aspects of the process. Direct CP violation, which is expected to be very small in the SM, can be tested by comparing the decay rates for B to \bar{B} :

$$A_{CP} \equiv \frac{\mathcal{B}(\bar{B} \rightarrow \bar{K}^{(*)}\ell^+\ell^-) - \mathcal{B}(B \rightarrow K^{(*)}\ell^+\ell^-)}{\mathcal{B}(\bar{B} \rightarrow \bar{K}^{(*)}\ell^+\ell^-) + \mathcal{B}(B \rightarrow K^{(*)}\ell^+\ell^-)}$$

The recent $BABAR$ analysis reports:

$$A_{CP}^K = -0.18_{-0.18}^{+0.18} \pm 0.01,$$

$$A_{CP}^{K^*} = 0.01_{-0.15}^{+0.16} \pm 0.01.$$

A lepton-flavor asymmetry (test of μ - e universality) can be defined by the ratio:

$$R \equiv \frac{\mathcal{B}(B \rightarrow K^{(*)}\mu^+\mu^-)}{\mathcal{B}(B \rightarrow K^{(*)}e^+e^-)}.$$

Models that would enhance $B_s \rightarrow \mu^+\mu^-$, such as SUSY with a Higgs at large $\tan\beta$, would also enhance R somewhat. At the current level of statistics, the test is not very restrictive, but is consistent with the SM expectation of unity. The recent $BABAR$ results are (for $q^2 > 0.1 \text{ GeV}^2$):

$$R_K = 0.96_{-0.34}^{+0.44} \pm 0.05,$$

$$R_{K^*} = 1.37_{-0.40}^{+0.53} \pm 0.09.$$

The most interesting and potentially important recent results address the isospin asymmetry, which compares the decay of neutral to charged B 's:

$$A_I \equiv \frac{\mathcal{B}(B^0 \rightarrow K^{(*)0}\ell^+\ell^-) - r\mathcal{B}(B^\pm \rightarrow K^{(*)\pm}\ell^+\ell^-)}{\mathcal{B}(B^0 \rightarrow K^{(*)0}\ell^+\ell^-) + r\mathcal{B}(B^\pm \rightarrow K^{(*)\pm}\ell^+\ell^-)},$$

where $r = \tau_0/\tau_+$ is the ratio of B^0 to B^+ lifetime. The value of A_I is expected to be close to zero in the SM, although at low- q^2 some deviation is expected (up to about 10%); in particular, the sign of this deviation depends on the sign of \tilde{C}_7 [3]. Figure 3 shows the A_I result in the two q^2 -bins in the recent *BABAR* analysis. A significant deviation from zero is observed in the low- q^2 bin for both K and K^* ($\sim 3\sigma$ in each case).

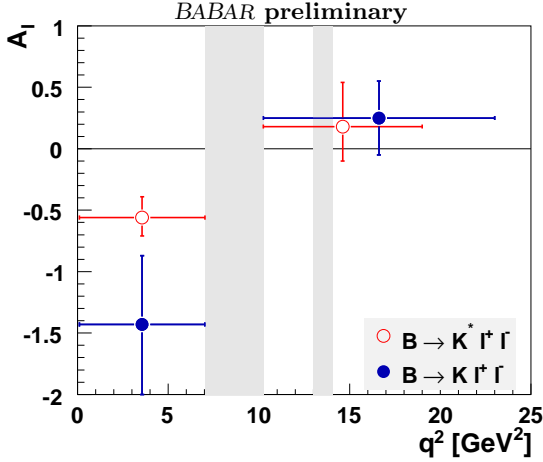


FIG. 3: The isospin asymmetry versus q^2 from *BABAR*: $B \rightarrow K\ell^+\ell^-$ (solid dots, blue); $B \rightarrow K^*\ell^+\ell^-$ (open circles, red).

The underlying fits to m_{ES} distributions for the low- q^2 bin are shown in Figure 4. The corresponding partial branching fractions are (for $0.1 < q^2 < 7.02 \text{ GeV}^2$):

$$\mathcal{B}(B^\pm \rightarrow K^\pm\ell^+\ell^-) = (2.5 \pm 0.5 \pm 0.1) \times 10^{-7},$$

$$\mathcal{B}(B^0 \rightarrow K^0\ell^+\ell^-) < 0.9 \times 10^{-7} \text{ (90\% CL)},$$

$$\mathcal{B}(B^\pm \rightarrow K^{*\pm}\ell^+\ell^-) = (9.8_{-2.4}^{+2.6} \pm 0.6) \times 10^{-7},$$

$$\mathcal{B}(B^0 \rightarrow K^{*0}\ell^+\ell^-) = (2.6_{-1.0}^{+1.1} \pm 0.2) \times 10^{-7}.$$

Subsequent to HQL08, Belle presented A_I measurements based on a 625 fb^{-1} dataset at ICHEP08 [4]. Belle's new results also indicate negative A_I values for q^2 below the J/ψ , but Belle observes less pronounced deviations from unity than *BABAR*. Negative A_I values at low q^2 tends to favor a flipped-sign for \tilde{C}_7 .

C. Angular Analysis

Angular distributions as functions of q^2 , particularly the forward-backward lepton asymmetry A_{FB} , are particularly sensitive to possible new physics. This asymmetry, defined as follows, basically measures the

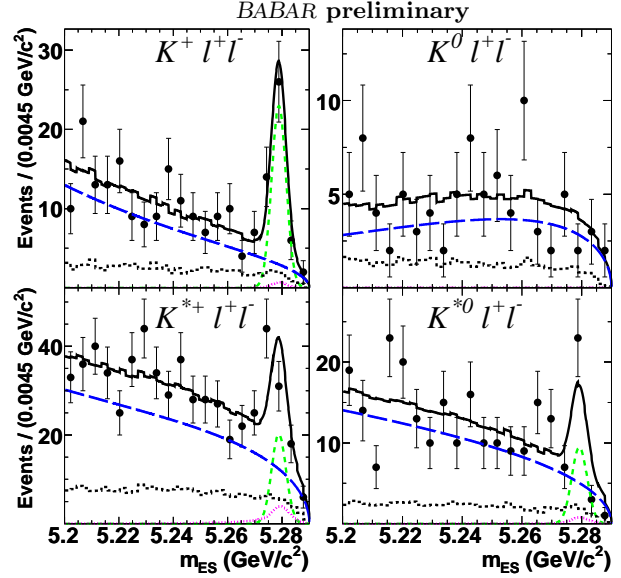


FIG. 4: m_{ES} distributions for the low- q^2 bin: $K^\pm\ell^+\ell^-$ (upper left); $K^0\ell^+\ell^-$ (upper right); $K^{*\pm}\ell^+\ell^-$ (lower left); $K^{*0}\ell^+\ell^-$ (lower right). Fit results are superimposed: full fit (solid blue), signal (black dashed), combinatorial background (magenta dashed), misidentified muons (green dotted), peaking backgrounds (red dotted).

tendency of the $\ell^+(\ell^-)$ to be in the same hemisphere as the $\bar{B}(B)$ when viewed from the dilepton rest frame:

$$A_{FB}(q^2) = \frac{1}{\frac{d\Gamma}{dq^2}} \int_{-1}^1 d\cos\theta_l \frac{d^2\Gamma}{dq^2 d\cos\theta_l} \text{sgn}(\cos\theta_l),$$

where Γ is the $B \rightarrow K^*\ell^+\ell^-$ decay width and θ_l is the angle between the ℓ^- and B in the $\ell^+\ell^-$ rest frame.

An additional angular variable of importance is the fraction of longitudinal K^* polarization, F_L . The quantity F_L has some sensitivity to new physics and also affects the angular distributions of θ_l which must be fit to determine A_{FB} . Extraction of F_L and A_{FB} from $B \rightarrow K^*\ell^+\ell^-$ candidate events requires an understanding of the angular correlations of background events. These can be studied using $B \rightarrow K^*\mu^\pm e^\mp$ events in data, as well as Monte Carlo simulations. The analysis procedure and fitting method can be validated using the $B \rightarrow J/\psi[\psi(2s)]K^*$ control samples discussed earlier. In addition, a null result for A_{FB} is expected in $B \rightarrow K\ell^+\ell^-$, providing another check.

BABAR performs a three-step procedure, the results of which are shown in Figure 5. The first fit determines signal and background yields; the second determines F_L ; and the third determines A_{FB} . The results, in the low- and high- q^2 bins, are:

$$F_L^{\text{low}} = 0.35 \pm 0.16 \pm 0.04,$$

$$F_L^{\text{high}} = 0.71_{-0.22}^{+0.20} \pm 0.04,$$

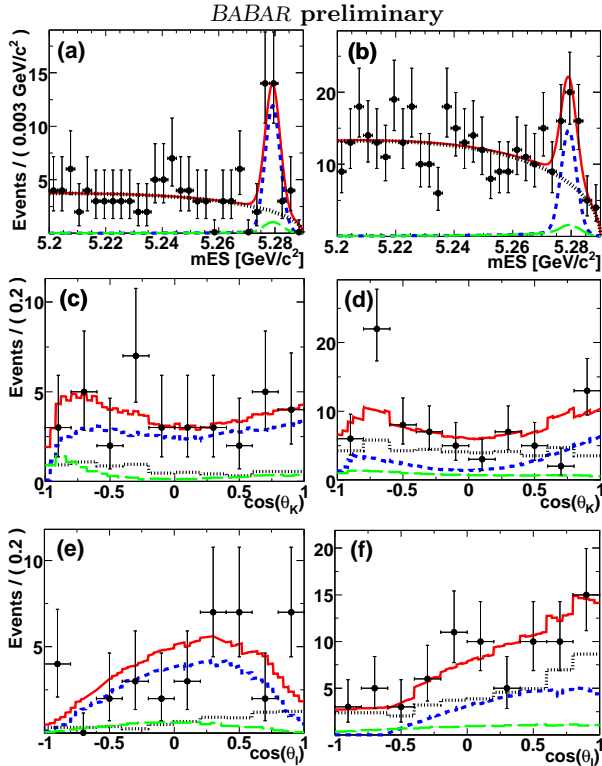


FIG. 5: *BABAR* fit results for determining F_L and A_{FB} in two q^2 bins. (a) and (b) m_{ES} distributions in low- and high- q^2 bins, respectively, used to fit signal and background yields; (c) and (d) $\cos\theta_K$ distributions fit to determine F_L ; (e) and (f) $\cos\theta_l$ distributions fit to determine A_{FB} . The total fit is shown in red (solid); signal in blue (dashed); combinatorial background in black (dots); and peaking backgrounds in green (long dashes).

$$A_{FB}^{\text{low}} = 0.24_{-0.23}^{+0.18} \pm 0.05,$$

$$A_{FB}^{\text{high}} = 0.76_{-0.32}^{+0.52} \pm 0.07.$$

Obviously these results are statistically limited, even in two q^2 bins. Nonetheless, they can be compared with SM expectations. Figure 6 shows the F_L measurements along with the SM expectation, as well as a flipped- \tilde{C}_7 scenario.

The A_{FB} results are shown in Figure 7, which overlays the recent *BABAR* results on prior Belle results [5]. The *BABAR* and Belle results are consistent, and tend to favor positive values of A_{FB} , particularly at large q^2 . This disfavors the models, shown in Figure 7, with the sign of $\tilde{C}_9\tilde{C}_{10}$ flipped. Subsequent to HQL08, Belle presented updated A_{FB} results [4] based on 625 fb^{-1} at ICHEP08; the updated results are consistent with the prior Belle results and the recent *BABAR* results.

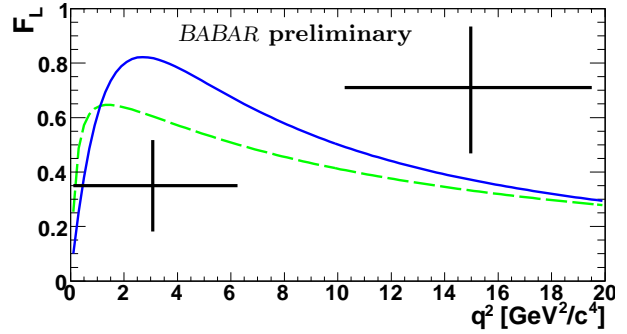


FIG. 6: *BABAR* F_L results in two q^2 bins. The solid (blue) line is the SM expectation. The dashed green line shows a flipped-sign \tilde{C}_7 model.

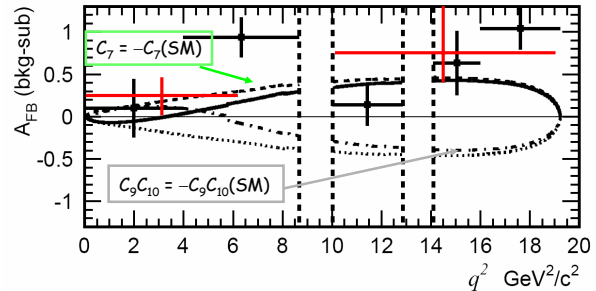


FIG. 7: *BABAR* Preliminary *BABAR* A_{FB} results in two q^2 bins in red. The black points are from Belle [5]. The solid black curve is the SM expectation. The dashed curve shows a flipped-sign \tilde{C}_7 model. The dotted curve and the dot-dashed curve show models with the sign of $\tilde{C}_9\tilde{C}_{10}$ flipped.

III. SEARCHES FOR $B \rightarrow \pi\ell^+\ell^-$

Belle recently reported a new search for $B \rightarrow \pi\ell^+\ell^-$ based on 657 million $B\bar{B}$ pairs (about 607 fb^{-1}) [6]. Continuum and semileptonic B decay backgrounds are suppressed using likelihood ratios that combine event shape, vertex, and other information. Two-dimensional maximum likelihood fits are performed in the variables ΔE and m_{bc} . No signals are observed and 90% confidence level limits are set on $B^+ \rightarrow \pi^+\ell^+\ell^-$ and $B^0 \rightarrow \pi^0\ell^+\ell^-$, as well as an isospin-averaged combination of the two. These new limits are listed in Table I, along with previous limits from *BABAR* [7]. The table also includes SM expectations [8]. It is noteworthy that the Belle upper limit on $B^+ \rightarrow \pi^+\ell^+\ell^-$ is approaching the expected SM branching fraction.

TABLE I: Upper limits (90% CL) on $\mathcal{B}(B \rightarrow \pi \ell^+ \ell^-)$ from Belle and BABAR, along with SM expectations.

Mode	SM	Belle	BABAR
$B^+ \rightarrow \pi^+ \ell^+ \ell^-$	3.3×10^{-8}	$< 4.9 \times 10^{-8}$	$< 12 \times 10^{-8}$
$B^0 \rightarrow \pi^0 \ell^+ \ell^-$	1.7×10^{-8}	$< 15.4 \times 10^{-8}$	$< 12 \times 10^{-8}$
$B \rightarrow \pi \ell^+ \ell^-$	3.3×10^{-8}	$< 6.2 \times 10^{-8}$	$< 9.1 \times 10^{-8}$

IV. SEARCHES FOR $B \rightarrow K^{(*)} \nu \bar{\nu}$

With missing neutrinos, $B \rightarrow K^{(*)} \nu \bar{\nu}$ decays are particularly difficult to isolate, and backgrounds are daunting. To clean up events, both BABAR and Belle have performed these searches by requiring one B in the event to be fully reconstructed, thereby removing continuum events and making it possible to assign particles in the event either to the tag B or the signal candidate. BABAR has reported recent results for both $B \rightarrow K \nu \bar{\nu}$ (based on 319 fb^{-1}) and $B \rightarrow K^* \nu \bar{\nu}$ (based on 413 fb^{-1}) in separate analyses, both of which rely on reconstructing one B via $B \rightarrow D^{(*)} \ell \nu$. The $B \rightarrow K \nu \bar{\nu}$ search utilizes a Random Forest algorithm [9] to separate signal and background, while the $B \rightarrow K^* \nu \bar{\nu}$ analysis utilizes a maximum likelihood fit that relies on the differences in distribution of extra energy in the event between signal and background. The results from these searches are listed in Table II, along with the SM expectations [10] and the current Belle limits [11].

TABLE II: Upper limits (90% CL) on $\mathcal{B}(B \rightarrow K^{(*)} \nu \bar{\nu})$ from Belle and BABAR, along with SM expectations. The BABAR results are preliminary.

Mode	SM	Belle	BABAR
$B^+ \rightarrow K^{*+} \nu \bar{\nu}$	1.3×10^{-5}	$< 14 \times 10^{-5}$	$< 9 \times 10^{-5}$
$B^0 \rightarrow K^{*0} \nu \bar{\nu}$	1.3×10^{-5}	$< 34 \times 10^{-5}$	$< 21 \times 10^{-5}$
$B^+ \rightarrow K^+ \nu \bar{\nu}$	0.4×10^{-5}	$< 1.4 \times 10^{-5}$	$< 4.2 \times 10^{-5}$
$B^0 \rightarrow K^0 \nu \bar{\nu}$	0.4×10^{-5}	$< 16 \times 10^{-5}$	

V. SEARCHES FOR $B^0 \rightarrow \ell^+ \ell^-$

While these decays are sensitive to the same electroweak penguin and W -box diagrams as the other decays discussed above, the prospects of observing them at the SM level are rather remote. The decay $B^0 \rightarrow \tau^+ \tau^-$ is experimentally very challenging due to the difficulties associated with multiple missing neutrinos. And while the experimental signatures of $B^0 \rightarrow \mu^+ \mu^-$ and $B^0 \rightarrow e^+ e^-$ are nearly ideal, these decays are helicity suppressed to levels that make them inaccessible for the B -factories.

The SM branching fractions are expected to be about 10^{-7} for $\tau^+ \tau^-$, 10^{-10} for $\mu^+ \mu^-$, and 10^{-15} for $e^+ e^-$. Non-SM scalar interactions would not be helicity suppressed, so that there is a window for new physics above the SM level. Thus, it is worthwhile to search for these modes even though the SM level remains inaccessible. The most promising opportunity, particularly for the $\mu^+ \mu^-$ mode (including $B_s \rightarrow \mu^+ \mu^-$), occurs at hadron colliders where the large hadronic B -production cross section provides a major advantage. Table III summarizes the current status of these modes.

TABLE III: Upper limits (90% CL) on $\mathcal{B}(B^0 \rightarrow \ell^+ \ell^-)$ from Belle, BABAR, and CDF.

Mode	Belle	BABAR	CDF
$\tau^+ \tau^-$		$< 4.1 \times 10^{-3}$ [12]	
$\mu^+ \mu^-$	$< 1.6 \times 10^{-7}$ [13]	$< 5.2 \times 10^{-8}$ [14]	$< 1.8 \times 10^{-8}$ [15]
$e^+ e^-$	$< 1.9 \times 10^{-7}$ [13]	$< 1.1 \times 10^{-7}$ [14]	

VI. SEARCHES FOR $B^+ \rightarrow \ell^+ \nu$

$B^+ \rightarrow \ell^+ \nu$ decays would occur via the tree-level exchange of a W -boson. The branching fractions are precisely predictable in the SM given the relevant CKM factor, $|V_{ub}|$, and the B -meson decay constant f_B . $|V_{ub}|$ is best measured in $b \rightarrow u \ell \nu$ semileptonic decays; a review of the latest measurements can be found in this proceeding [16].

Considerable progress has been made by both Belle and BABAR toward measurements of $B^+ \rightarrow \tau^+ \nu$. This is the topic of another contribution to this proceeding[2] and will not be discussed here. Table IV summarizes the status of the other modes. It is noteworthy that Belle, using 253 fb^{-1} , has set a limit in the $\mu \nu$ mode that is within about a factor of three of the SM expectation [17]. Thus, this mode appears likely to be just beyond the reach of the current B -factory experiments.

TABLE IV: Upper limits (90% CL) on $\mathcal{B}(B^+ \rightarrow \ell^+ \nu)$ from Belle[17] and BABAR [18], along with SM expectations.

Mode	SM	Belle	BABAR
$B^+ \rightarrow \mu^+ \nu$	$\sim 5 \times 10^{-7}$	$< 1.6 \times 10^{-6}$	$< 6.6 \times 10^{-6}$
$B^+ \rightarrow e^+ \nu$	$\sim 1 \times 10^{-11}$	$< 9.8 \times 10^{-7}$	

VII. CONCLUSION

The rare FCNC decays discussed here are among the most interesting in B physics. Considerable exper-

imental progress has been made by Belle and *BABAR*. Yet, a common theme emerges from this discussion of several different modes. It is the need for more data.

Significant and probing measurements have become possible in decays involving the $b \rightarrow s\ell^+\ell^-$ transition, but the results are statistically limited. The results reported thus far do not utilize the full data sets of *BABAR* or Belle (for which the ultimate data set will be much larger), but even so, the final results from *BABAR* and even Belle will clearly still be statistics limited. Other interesting processes such as $B^+ \rightarrow \pi^+\ell^+\ell^-$ and perhaps $B^+ \rightarrow \mu^+\nu$ are just beyond the reach of the existing *B*-factories. To do this physics

justice, it seems apparent that a dataset of at least 10 ab^{-1} is needed. This is one of a number of strong arguments that make up the physics case for “super” *B*-factories.

Acknowledgments

I would like to thank G. Eigen and K. Flood for useful input.

-
- [1] G. Eigen, Proceedings of FPCP 2008, arXiv: 0807.4076 [hep-ex]
- [2] M. Barrett, this proceeding.
- [3] Th. Feldman and J. Mattias, JHEP 0301, 074 (2003).
- [4] I. Adachi *et al.*, BELLE-CONF-0822, arXiv:0810. 0335.
- [5] A. Ishikawa *et al.*, Phys. Rev. Lett. **96**, 251801 (2006).
- [6] J.-T. Wei *et al.*, Phys. Rev. D **78**, 011101 (2008).
- [7] B. Aubert *et al.*, Phys. Rev. Lett. **99**, 051801 (2007).
- [8] T.M. Aliev and M. Savci, Phys. Rev. D **60**, 014005 (1999).
- [9] L. Breiman, Random Forests, Machine Learning **45**, 5-32 (2001); <http://www.stat.berkeley.edu/~breiman/RandomForests>
- [10] G. Buchalla *et al.*, Phys. Rev. D **63**, 014015 (2000).
- [11] K.-F. Chen *et al.*, Phys. Rev. Lett. **99**, 221802 (2007).
- [12] B. Aubert *et al.*, Phys. Rev. Lett. **96**, 241802 (2006).
- [13] M.-C. Chang *et al.*, Phys. Rev. D **68**, 111101 (2003).
- [14] B. Aubert *et al.*, Phys. Rev. D **77**, 032007 (2008).
- [15] T. Aaltonen *et al.*, Phys. Rev. Lett. **100**, 101802 (2008).
- [16] A. Petrella, this proceeding.
- [17] Phys. Lett. B **647**, 67 (2007).
- [18] B. Aubert *et al.*, Phys. Rev. Lett. **92**, 221803 (2004).